Response to Robert Tycko (Editor)

Reviewer comments are in black, responses are in blue

This manuscript is potentially suitable for publication in Magnetic Resonance after the authors make revisions that fully address the comments of the two anonymous reviewers as well as the following points:

1. The "tennis racquet theorem" says that any object in free space will rotate stably about axes close to its smallest and largest principal axes of inertia, but not stably around the middle axis of inertia. This is also mentioned by one of the anonymous reviewers. The authors should explain how this relates to their statement that "an object is capable of spinning stably about ANY axis ... as long as there are no avenues to dissipate rotational energy." The authors' statement seems erroneous, except perhaps because they are discussing situations where the object is not in free space. Their later statement that "a high aspect ratio cylindrical MAS rotor requires active stabilization...in order to spin stably about its axis of symmetry" also appears to contradict the tennis racquet theorem.

This statement was in error. This was meant to say "an axially-symmetric object is capable of spinning stably about any axis," but it turns out that this statement is also erroneous. We have removed this statement and instead included in the manuscript a discussion with respect to the conditions of stability associated with axially symmetric objects. Using Euler's equations, one can show that a rigid, axially-symmetric object spins stably about its axis of symmetry regardless of whether the moment of inertia about that axis is the greatest or smallest moment. However, due to energy dissipation phenomena, objects tend to prefer to rotate about the axis with the highest moment of inertia.

2. The examples of satellites and asteroids may not be relevant to an MAS rotor. I suspect the behavior of satellites and asteroids may be affected by INTERNAL dissipation (movement of internal material), which is not an issue for an MAS rotor. This may need clarification.

Avenues to dissipate energy in the vacuum of space must necessarily concern internal dissipation, as there is no surrounding medium to which the rotational energy can be dissipated. However, in the MAS stator, the surrounding gas dissipates rotational energy. The operating principle of pneumatic MAS depends on energy transfer between the gas and the rotor. We have clarified this point in our discussion.

3. A potential problem with spherical rotors may be that the magic angle needs to be readjusted for each sample, in other words the final direction of the axis of rotation may depend on the mass distribution within the rotor or on imperfections in the rotor itself. Is this true? The authors should comment on this issue, one way or the other.

Once adjusted to the proper angle for one rotor, a second rotor will spin at an angle very close to the magic angle, but not exactly. This is definitely a current challenge with the method, and something we are currently working on addressing. For now, it is recommended that all samples include some KBr to readjust the angle as needed, but we plan to solve this issue in an upcoming manuscript.

4. The description that "the nozzle aperture is placed at the complement of the magic angle in order to tilt the spinning axis of the rotor to a value near the magic angle" needs further clarification. A more detailed drawing of the stator in Figure 1 might help.

Figure 1 has been updated to show a cross section of the stator from another angle. We hope this addresses the concern.

Response to Anonymous Referee #1

Reviewer comments are in black, responses are in blue

General Comments:

The authors discuss eight different turbine groove designs for spherical magic angle spinning rotors. They find that deep turbine grooves do not allow stable spinning, and that some shallow groove designs allow modest increases in spinning speed compared to a groove-free surface. The stability of these spherical ring rotors is discussed in terms of the rotor's principle moments of inertia, and compared to the situation for more conventional cylindrical MAS rotors.

The paper reports progress on the optimization of the very novel magic angle spinning rotor system design that has come out of this laboratory in recent years, and gives a theoretical basis for why the stability of this design is so robust.

The results reported here represent a necessary step in the evolution and optimization of this new spinning system design. While the community of researchers who build their own magic angle spinning systems is rather small, and those who spin with spherical rotors is smaller still, this work represents what I hope will be one of many modest forward steps that will eventually make spherical rotors a compelling alternative to conventional designs.

The paper is logically organized and easy to follow.

Specific comments:

The title seems inappropriate for the work described. While I understand that the fact that groove less rotors perform nearly as well as the best grooved design is one of the significant results, the title ignores most of the experiments described.

While we initially wanted to highlight the most interesting result in our title, we agree that the title as written does have the potential to overshadow the other experiments and discussion. Unless there are restrictions on changing the title after the discussion period, we have proposed a title change to "Highly Stable Magic Angle Spinning Spherical Rotors," in order to de-emphasize the focus on the rotor lacking turbine grooves and instead focus more broadly on the discussion of stability.

In considering moments of inertia, the authors consider empty rotors: spherical rings or cylindrical shells. But some conventional cylindrical rotor designs do not spin well empty - the sample matters. The addition of the sample is considered only cursorily at the end of the manuscript. Presumably if the sample density is much less than the density of the rotor itself things aren't changed much by the sample, but maybe something more could be said?

To address this concern, we have added as supplementary material an interactive Mathematica document which allows the reader to independently adjust the densities for the sample, caps, and rotor in order to see the effect on the moments of inertia as a function of normalized inner radius. We have added additional discussion on this topic to this document.

The discussion of the stability of rotation is somewhat unsatisfying. There is a commonly known theorem about rotation that for objects with three distinct moments of inertia, rotations about the axes having the largest and smallest moments are stable, while

rotation about the intermediate axis is not (tennis rackets are a prototypical example). That theorem would suggest that cylinders rotating about their long axes should be stable, as long as both energy and angular momentum are conserved. The situation with both spherical rings and cylinders might be a little different because of the cylindrical symmetry, where there is no intermediate axis. I'd like to see a bit deeper discussion of the stability criteria. While this represents old physics, it would be nice to see a sound discussion in the context of magic angle spinning systems.

We have taken this comment to heart and have now added a discussion with respect to the conditions of stability associated with axially symmetric objects. Using Euler's equations, one can show that a rigid, axially-symmetric object spins stably about its axis of symmetry regardless of whether the moment of inertia about that axis is the greatest or smallest moment. However, due to energy dissipation phenomena, objects tend to prefer to rotate about the axis with the highest moment of inertia.

I wonder if the statement on line 108, that rotation about any axis is stable if there is no energy dissipation, is actually helpful in understanding stability issues?

We have removed this statement in favor of a more rigorous discussion of the rotational dynamics.

Minor issues:

pg 2 line 46. What is meant by 4.7 M-ohm transimpedance amplifier? Does that mean a 4.7 M-ohm resistor in series with the photodiode?

The resistor in this case is in the feedback loop of the amplifier. The size of the feedback resistor relates to the gain of the amplifier and also determines the noise of the amplifier. We have adjusted the text to say "a transimpedance amplifier with a 4.7 M-Ohm feedback resistor" for clarity.

line 51 reference should be parenthesized.

This has now been corrected.

line 162, 175 and others: links to cited doi's appear twice in a number of the references.

We have now corrected these citations.

Response to Anonymous Referee #2

Reviewer comments are in black, responses are in blue

General Comments:

The authors examine and discuss factors important for fast, stable spinning of spherical rotors for magic angle spinning solid-state NMR experiments. They show that a stator for spherical rotors can be integrated into a commercial NMR probe head in a straightforward manner. They present measurements of spinning speeds and spinning stability achieved with eight different turbine groove designs, including one design with no grooves. The spinning rate achieved at a given pressure is shown to be sensitive to the surface grooves, with moderate spinning rate improvements observed for some groove geometries over others, and over a smooth rotor. Finally, they present a theoretical motivation for the spinning stability they observed in spherical rotors based on an analysis of the principal values of a spherical rotor's moment of inertia tensor.

The results presented here are broadly interesting to the solid-state NMR community. Spherical rotors represent an alternative to the conventionally used cylindrical rotors, with several potential benefits which the authors outline. While much development work is still necessary, this work reports progress which is likely to spur further investigation into spherical rotors, and into other alternative rotor designs.

Specific Comments:

It would be interesting to hear comments about how spherical rotor stability is influenced by the sample, beyond what was included at the end of the manuscript.

To address this concern, we have added as supplementary material an interactive Mathematica document which allows the reader to independently adjust the densities for the sample, caps, and rotor in order to see the effect on the moments of inertia as a function of normalized inner radius. We have added additional discussion on this topic to this document.

NMR data acquired on a sample spun in rotor H were acquired with a 3.5 kHz spinning speed, which is below the maximum spinning speed reported for rotor H in Figure 3a. Was 3.5 kHz chosen for stability reasons?

As shown in Figure 3A, rotor H is capable of spinning stably at 4 kHz at 4 bar of air pressure. However, we exercised reasonable caution for the NMR experiment, as 3.5 kHz can be achieved with nearly half the air pressure required to reach 4 kHz, and the experimental results achieve the same goal.

Was any consideration given when designing deep turbine grooves to how these grooves might alter the moment of inertia tensor of the spherical rotors?

At the time of their design, we were not considering that removing material might have a significant effect on the inertia tensor of the rotor itself, and instead assumed that the grooves would be a negligible change. However, it is possible that removing a significant amount of material from the outer equatorial region could have had an impact on their stability by changing the inertia tensor. We still maintain however, that the primary effect causing rotors E, F, and G to not spin stably was due to the excess space allowing for complex and turbulent fluid flows in the stator cup. The motion of rotors E, F and G in the

stator is random and chaotic even at very low pressures/flow rates, while for the other rotors, they simply don't spin until a certain pressure threshold is reached and then beyond that, spin up smoothly. More research is needed to explore the fluid dynamics of the gas flow within the stator cup, as even for the simplest case (Rotor H) we expect the fluid flow to be very complex and require a complete 3D description. For now, the guidance on turbine groove development is to make them as shallow as possible, which should also minimize changes to the spherical ring inertia tensor.

Technical corrections:

The formatting of several of the references is somewhat strange, with the doi appearing twice in multiple references.

We have now corrected this issue.

Response to Geoffrey Bodenhausen

Comments are in black, responses are in blue

It would be interesting to know if more than 5 rotors were tested, and if the performance documented in Fig. 3 refers to their average performance or to unique cases.

We tested all 8 rotors, however rotors E, F and G did not spin stably. Figure 3 refers to unique cases, but the results are reproducible to within ~100 Hz for each rotor at each pressure value. Collecting statistics is useful for our development of these rotors and stators, but the results can vary based on which printed stator is used and the exact conditions of the experimental setup. The figure shown represents a unique test series performed using the same stator and experimental conditions for all rotors, as described in the experimental details.

The description of the curves of Fig. 3 as “pressure increases at higher pressures less effectively increased at spinning rate than at lower pressure” should be replaced by a sober reference to the figure itself.

We agree that this sentence does not benefit the discussion and have removed it.

While the discussion of the moments of inertia for empty spherical and cylindrical rotors is interesting, it is only at the very end that the authors admit that the sample and caps will affect these considerations.

To address this concern, as other reviewers have also noted interest in this issue, we have added as supplementary material an interactive Mathematica document which allows the reader to independently adjust the densities for the sample, caps, and rotor in order to see the effect on the moments of inertia as a function of normalized inner radius. We have added additional discussion on this topic to this document. The model we use is a simple approximation of how we pack sample into the rotors, but should give a sense for the effects of sample and cap density on the moments of inertia of the overall packed rotor.

The sentence “adjusted until the rotor’s spinning axis was inclined to the magic angle, taken as the maximal number of rotor echoes in the time domain data” leaves me dumbfounded. Surely it is the decay of the envelope of the rotational echoes that could be taken as a measure for the adjustment of the magic angle.

In a practice, when setting the magic angle, the researcher usually looks to see if more echoes are visible beyond the noise level out to a certain time in the time domain data as the angle is adjusted. Perhaps we chose a bit too practical of a description. We have modified this sentence to read: “The stator's pitch angle was adjusted until the rotor's spinning axis was inclined to the magic angle, as observed by measuring the decay of rotor echoes out to 10 ms in the time domain data.”

The claim that “the fact that rotor H established a stable spinning axis about its own axis of symmetry” is interesting, but this hardly “shows that the grooves do not direct the rotor to spin about this axis, but rather the geometry of the rotor itself is responsible”. There is no evidence that the machining of the groves agrees with the geometry.

We have measured the rotors that were machined, and found them to be within the tolerance levels of our design specifications. If a rotor with no grooves spins stably about its own axis, it shows that the grooves are not required in order to spin stably. The reason

it spins stably about its own axis must be due to another factor, and that is the spherical-ring geometry of the rotor itself.

I have learned in a first-year physics course (at ETH!) that objects end up tumbling around the axis with the largest moment of inertia. I believe that this has been known since the XIXth, perhaps even since the XVIIIth century. It is unfortunate that the designers of “early spacecraft such as Explorer 1” were not aware of this phenomenon.

This is a very important issue, and there is a lot of confusion surrounding this topic (including for us as we have worked on writing and developing this manuscript!), as classical rotational dynamics is an issue which seems simple on first glance, but is actually quite complex and has received significant attention and development over the past century. Euler’s equations have been known since the 18th century, but they do not say anything about objects ultimately ending up spinning about the axis with the greatest moment of inertia. They predict that a rigid, axially-symmetric object will spin stably about its axis of symmetry regardless of whether the moment of inertia along that axis is the greatest or smallest moment. What happened with the Explorer 1 was that the satellite was intended to spin about its lowest inertia axis, which should have been fine if the object was rigid. However, due to avenues for dissipating rotational energy internally being present (antennas on the craft) the satellite began a precession which eventually turned into an end over end spin. The result of Explorer 1 spurred the further development of rigid-body rotational dynamics to account for this phenomenon. If avenues to dissipate rotational energy are present, the “stable” configuration initially predicted by Euler’s equations is no longer stable. In MAS, a cylindrical rotor exchanges energy with the surrounding gas and can enter into a precession if it is not actively kept from doing so. This is partly why oversized bearings in the stator result in unstable spinning.

Response to Asif Equbal

Comments are in black, responses are in blue

I have two concerns regarding this draft.

1. Figure 4A shows that as the inner radius (r) in a sphere increases, the moment of inertia along Iz and Ix(or Iy) become unequal, with inertia along Iz being larger than Ix. The authors have used this fact to support the spinning-stability of sphere without groves. The moment of inertia of a sphere is proportional to the radius of sphere (R). Therefore, the absolute difference between the inertia in two directions (z and x) is also proportional to R. In the case presented, the sphere is large 9.5mm (with the maximum speed of~4-5 kHz), and therefore it has a preferred axis of rotation. But as one goes for smaller sphere to achieve faster spinning (which is a major goal here), the absolute difference between Iz and Ix will be smaller and smaller. And in such scenario, the spinning along any particular axis will not be stable.

All calculations were performed without using a fixed value for the radius. The results depicted in Figure 4 are valid for any given radius- note that the x-axis is “normalized inner radius,” which takes into account the fact that these results scale for any outer radius value. It is true that the absolute values of the moments of inertia will decrease with smaller rotors, but the ratio of values between Iz and Ix will always be the same. The size of the rotor should not affect these stability considerations. For experimental proof of this, we have spun 4mm spherical rotors stably at 28 kHz, and 2mm rotors at around 60 kHz (unpublished).

2. The authors have compared two cases, a sphere vs. a cylinder in figure 4. Sphere(hollow one) has preference to spin along "z" and a cylinder along "x". Using this simple comparison, authors have shown why a sphere is better than cylinder for stability. In reality, the sample cup should be viewed as a combination of coaxial: (i). Spherical ring, (ii) a hollow cylinder (in which sample will be filled), (iii) a solid cylinder (basically the sample filled in the cylinder) and (iv) curved cap. Different components (i, ii, iii and iv) will have different inertia. These are known or at least easy to calculate. Since moments of inertia are additive, it is possible to do a more realistic calculation, taking into consideration moments of inertia of all these components.

To address this concern, as other reviewers have also noted interest in this issue, we have added as supplementary material an interactive Mathematica document which allows the reader to independently adjust the densities for the sample, caps, and rotor in order to see the effect on the moments of inertia as a function of normalized inner radius. We have added additional discussion on this topic to this document. The model we use is a simple approximation of how we pack sample into the rotors, but should give a sense for the effects of sample and cap density on the moments of inertia of the overall packed rotor.

Minor concern: Authors have used same notations to represent the dimensions of the two objects. It is better to use distinguished symbols to , e.g., r_s, R_s, r_c and R_c.

For the results to be compared between the sphere and cylinder for a given outer radius R and inner radius r, we have chosen not to demarcate these with distinguished symbols.

Highly Stable Magic Angle Spinning Spherical Rotors~~Lacking Turbine Grooves~~

Thomas M. Osborn Popp[1], Alexander Däpp[1], Chukun Gao[1], Pin-Hui Chen[1], Lauren E. Price[1], Nicholas H. Alaniva[1], and Alexander B. Barnes[1]

[1]Laboratory for Physical Chemistry, ETH Zürich, Vladimir-Prelog-Weg 2, 8093 Zürich, Switzerland

Correspondence: Alexander Barnes (alexander.barnes@phys.chem.ethz.ch)

Abstract. The use of spherical rotors for magic angle spinning offers a number of advantages including improved sample exchange, efficient microwave coupling for dynamic nuclear polarization nuclear magnetic resonance (NMR) experiments and, most significantly, high frequency and stable spinning with minimal risk of rotor crash. Here we demonstrate the simple retrofitting of a commercial NMR probe with MAS spheres for solid-state NMR. We analyze a series of turbine groove geometries to investigate the importance of the rotor surface on spinning performance. Of note, rotors lacking any surface modification spin rapidly and stably even without feedback control. The high stability of a spherical rotor about the magic angle is shown to be dependent on its inertia tensor rather than the presence of turbine grooves.

1 Introduction

Magic angle spinning (MAS) nuclear magnetic resonance (NMR) is usually used for high resolution analysis of the local chemical environments of nuclear spins within biomolecular and inorganic solids (**??????????????**). The sample is spun rapidly about an axis inclined at the magic angle, which is 54.74° with respect to the external magnetic field B_0. This averages terms in the NMR Hamiltonian whose orientational dependence is described by the second-order Legendre polynomial $3\cos^2\theta - 1$ (**???**). For spins-$1/2$, MAS can yield spectra with highly resolved isotropic chemical shifts.

MAS has traditionally been performed by spinning a cylindrical rotor within a stator installed at the magic angle, thereby requiring a gas bearing to stabilize the rotor and drive gas to apply torque (**???**). However, we recently showed that it is possible to spin samples via a different paradigm, namely using spherical rotors spun using a single gas stream for both the bearing and drive (**??**). This approach allows highly stable rotor spinning about a single axis inclined at the magic angle, with record rates as high as 4.6 kHz (N_2, 4.1 Bar) and 10.6 kHz (He, 11 Bar) for 9.5 mm diameter rotors and 11.4 kHz (N_2, 3.1 Bar) and 28 kHz (He, 7.6 Bar) for 4 mm diameter rotors. Decreasing the rotor diameter permits even higher spinning rates. Additional benefits of spherical rotors include easy sample exchange and improved microwave access for dynamic nuclear polarization (DNP)-NMR experiments, yielding improved microwave B_1 field strength and homogeneity compared with current methods (**??**).

In order to make spherical rotors robust and accessible for magnetic resonance experiments and to design apparatuses capable of achieving very high MAS rates, we examined the spinning and stabilization mechanisms of these spherical rotors.

Here we: (i) demonstrate how a stator for spinning spheres can be easily integrated into a commercial NMR probehead, and (ii) examine the spinning behavior of a series of spherical rotors with various turbine groove geometries. We show that the spinning performance of spherical rotors can be improved by using a turbine groove geometry similar to the drive tips used in conventional cylindrical rotor MAS systems, which are themselves based on the Pelton impulse turbine (**?**). However, we also find across a wide array of turbine styles that spinning performance is remarkably indifferent to the surface design and that even a rotor without turbine grooves can achieve stable, on-axis spinning. We show that a spherical rotor attains its stability from its inherent shape and mass distribution (i.e., its inertia tensor) and that turbine grooves are not essential for stable spinning.

2 Experimental Apparatus

The experimental apparatus is depicted in Figure 1. The stator employed for spinning spherical rotors was designed to adapt into a double-resonance APEX-style Chemagnetics probe (built decades ago for spinning 7 mm diameter cylindrical rotors) and 3D printed in clear acrylonitrile-butadiene-styrene (ABS) using either a ProJet MJP2500 3D printer (3D Systems, Rock Hill, SC, US) or a Form3 3D printer (Formlabs, Somerville, MA, US). A double saddle coil made from 1.5 mm silver-coated copper magnet wire was wound by hand using a mandrel and wrapped in Teflon tape for insulation with the leads soldered into place in the existing RF circuit of the Chemagnetics probe. The two optical fibers of the tachometer system were introduced into holes at the bottom of the semi-transparent stator. The transceiver of the original tachometer system was replaced with a more sensitive circuit. The transmitter in this circuit was an SFH756 light emitting diode fed with 42 mA of current. The detector comprised an SFH250 photodiode and a transimpedance amplifier with a 4.7 MΩ ~~transimpedance amplifier~~ feedback resistor followed by a gain block providing a voltage gain of 42. The magic angle adjustment was achieved by coupling the stator to the existing angle adjust rod in the probe.

NMR experiments were performed at 7.05 T using a Bruker Avance III spectrometer (Bruker Corp., Billerica, MA, US). ^{79}Br spectra were taken at a transmitter frequency of 75.46 MHz and a MAS rate of 3.5 kHz. The implementation of a double saddle coil within the probe enabled the application of a 35 kHz B_1 field on ^{79}Br with 300 W incident RF power, a significant improvement over our previous implementation of 9.5 mm spherical rotors, which achieved a B_1 field of only 12.5 kHz using a split coil and 800 W incident RF power ~~?~~(**?**).

The 9.5 mm spherical rotors were machined from yttria-stabilized zirconia (O'Keefe Ceramics, Woodland Park, CO, US). Seven new spherical rotor designs were introduced (Figure 2), each with a 2.54 mm inner diameter cylindrical through hole: notched (rotors A, C), Pelton-style (rotors B, F), circular (rotors C, G), dimpled (rotor D), and with no flutes (rotor H). For the notched, circular, and Pelton-style rotors, two variations were machined differing by 0.5 mm in depth. For spin testing, each rotor was filled with a rigid 3D printed cylindrical ABS blank terminated with 4.75 mm spherical radius contoured ends. For the NMR experiment, the rotor was packed with 97.1 mg KBr powder and sealed at each end with 3D printed ABS plugs. The same stator design was used for all spin testing experiments.

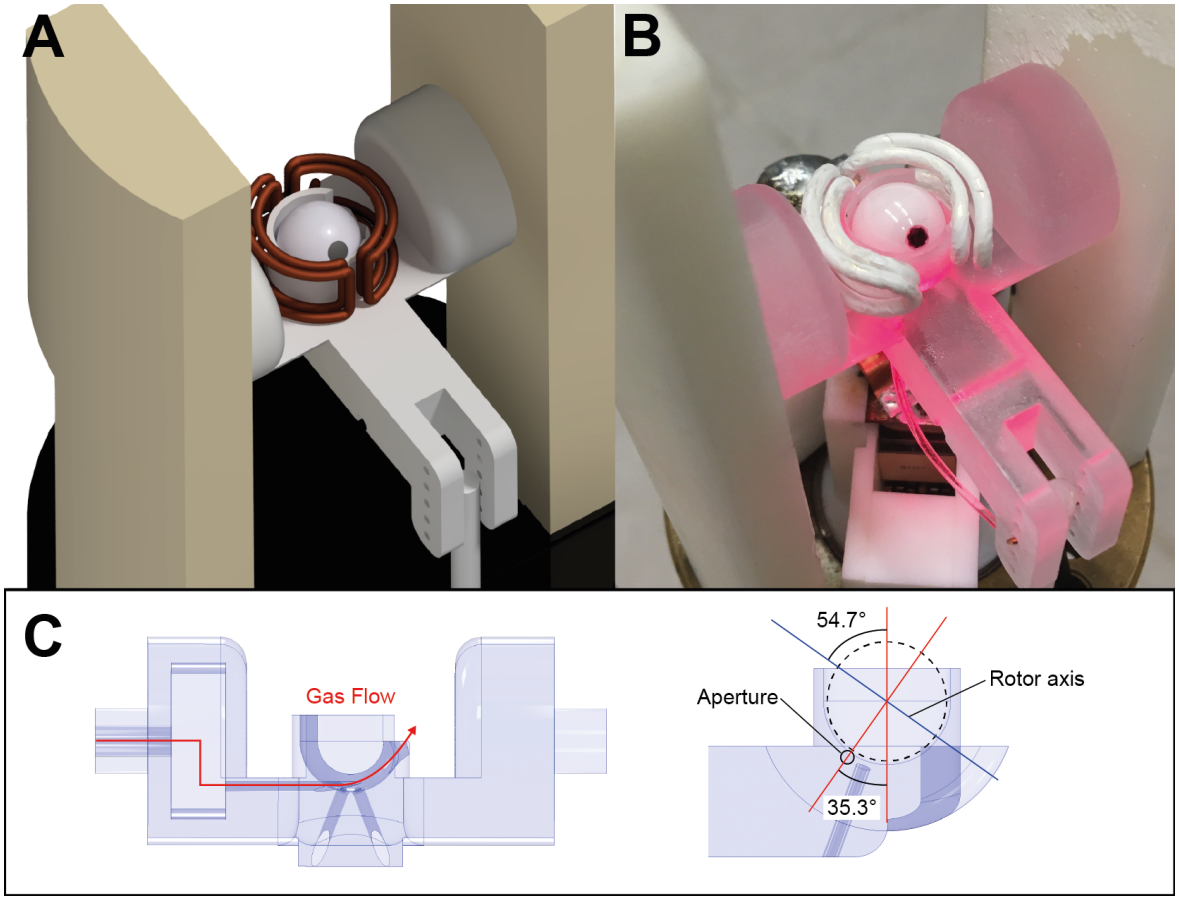

Figure 1. Experimental apparatus. A.) Probehead design schematic depicting the stator with a double saddle coil, spherical rotor, and angle adjust arm. B.) Fully assembled probehead. C.) Cross-section ~~view~~ views of the stator showing the drive gas inlet and angled through holes for the fiber optic tachometer. Drive gas is fed ~~from~~ through the ~~left side~~ nozzle aperture placed at the complement of the magic angle (35.3°) into the stator cup~~(red arrow)~~. ~~C.) Fully assembled probehead.~~

3 Results and Discussion

Spherical rotors spin within the hemispherical stator cup by the application of a gas stream along the rotor's equator from a converging nozzle tangent to the rotor surface (**?**). The nozzle aperture is placed at the complement of the magic angle (~~35.26~~35.3°) in order to tilt the spinning axis of the rotor to a value near the magic angle (as shown in Figure 1C). The rotor turbine grooves are intended to provide a means to efficiently couple the gas stream to the rotor surface, converting the kinetic energy of the fluid flow into rotational kinetic energy.

The designs depicted in Figure 2 were chosen to explore this concept. Intuition might suggest that deeper grooves allow for greater coupling to the gas stream due to the increased surface area perpendicular to the direction of fluid flow. However, the

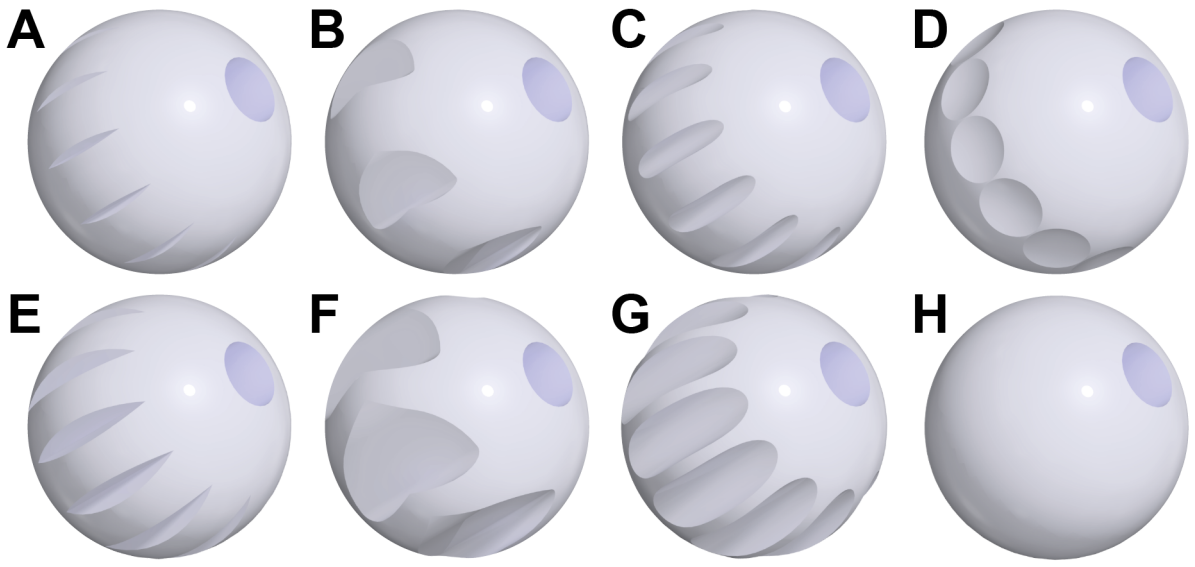

Figure 2. 9.5 mm spherical rotor turbine groove designs. Each rotor has a 2.54 mm diameter through hole. A.) Twelve 60º notched grooves, 0.35 mm depth (as described previously by **?**). B.) Six impeller-style grooves, 0.25 mm radius. C.) Twelve circular 0.25 mm radius grooves. D.) Twelve dimpled grooves, 4.75 mm radius dimples. E.) Twelve 60º notched grooves, 0.85 mm depth. F.) Six impeller-style grooves, 0.5 mm radius. G.) Twelve circular 0.5 mm radius grooves. H.) Smooth surface, no flutes machined.

deep-grooved rotors E, F, and G could not spin stably under any of the conditions tested. It is possible that the large spaces created by the removal of material to make these deep grooves allow chaotic and turbulent flows to develop within the stator cup. The shallow-grooved rotors A, B, C, and D, as well as rotor H, achieved stable spinning. Figure 3A shows the spin test data in air at gauge pressures ranging from 0 to 4.3 Bar for these five rotors. Across the five turbine geometries, the spinning rate increased non-linearly with respect to the applied pressure~~; pressure increases at higher pressures less effectively increased the spinning rate than at lower pressures~~. The maximum spinning rates for the five rotors at the pressures tested ranged between 4 and 6 kHz in air, with Pelton-style rotor B having the highest maximum spinning rate of 5.7 kHz. Note that the maximum tested pressure was not limited by the rotors, as their spinning rates would be predicted to increase with increasing pressure, but rather the maximum pressure was limited to ∼4 Bar due to safety concerns with regard to the connecting assemblies. Rotor B's maximum observed rate was a significant improvement over our previous maximum of 4.6 kHz for 9.5 mm rotors in air, which was achieved using rotor A at 4.1 Bar (**?**). As rotor A also performed better in our current tests, with a maximum rate of 5.2 kHz at 4.1 Bar, we attribute some of the performance gains to the higher precision 3D printing of our latest stators. However, the further increase to 5.7 kHz with rotor B is likely to be due to the Pelton-style grooves more efficiently coupling to the fluid flow~~and the rotor surface with a sufficiently shallow groove profile to prevent undesirable complex fluid flows in the stator~~.

A significant finding was that rotor H, with its smooth surface and lack of grooves, spun stably and on-axis. While not delivering the highest frequency spinning of the tested rotors, its performance was comparable to many of the designs with

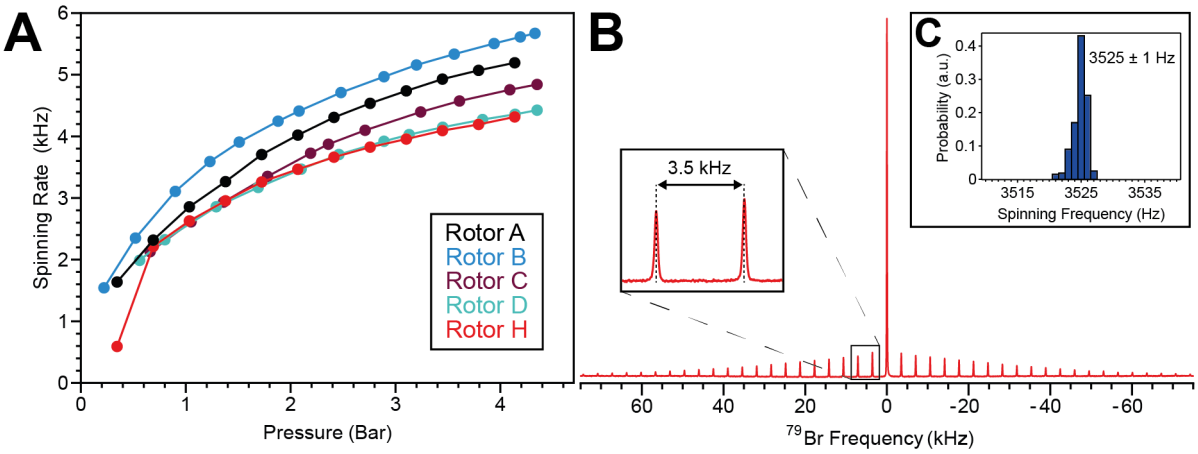

Figure 3. Spin test data. A.) Spinning rate as a function of applied air pressure for rotors A, B, C, D, and H. B.) ^{79}Br spectrum of KBr packed into rotor H and spinning at 3.5 kHz at the magic angle; 512 scans. C.) Histogram of spinning frequencies without spinning regulation over the 10 minute KBr data acquisition period.

machined grooves. Figure 3B shows the ^{79}Br spectrum of KBr at 3.5 kHz MAS using rotor H. The stator's pitch angle was adjusted until the rotor's spinning axis was inclined to the magic angle, ~~taken as the maximal number~~ as observed by measuring the decay of rotor echoes out to 10 ms in the time domain data. The spectrum shows the spinning sideband manifold equally spaced by 3.5 kHz, corroborating the spinning rate observed by optical tachometry. The spinning was stable, with a standard deviation of ± 1 Hz without the use of any spinning regulation mechanism (Figure 3C). The ability of rotor H to spin stably at reasonable MAS rates implies that while turbine grooves can improve fluid flow and rotor coupling, a significant contribution to the overall spherical rotor spinning mechanism is simply from the torque created by drag induced by the driving gas stream moving across the rotor surface. Additionally, the fact that rotor H established a stable spinning axis about its own axis of symmetry shows that the grooves do not direct the rotor to spin about this axis, but rather that the geometry of the rotor itself ~~is~~ must be responsible.

A spherical rotor with a cylindrical through hole is a solid known as a spherical ring. The ~~inertia tensor~~ moments of inertia for a spherical ring of constant density ρ, outer radius R, and inner radius r, where $R \geq r$ and z lies along the axis of ~~cylindrical symmetry, is~~ symmetry, are given by:

$$I_x^{sr} = I_y^{sr} = \frac{4}{15}\pi\rho(R^2 - r^2)^{3/2}\left(\frac{4R^2 + r^2}{2}\right) \tag{1}$$

~~Considering~~

$$I_z^{sr} = \frac{4}{15}\pi\rho(R^2 - r^2)^{3/2}(2R^2 + 3r^2) \tag{2}$$

As most previous MAS experiments have been performed with cylindrical rotors, it is worth examining the inertia tensor of a cylindrical shell for comparison. For a cylindrical shell of constant density ρ, outer radius R, inner radius r, and length of $2kR$, where k is the aspect ratio and $R \geq r$, the ~~inertia tensor is~~ moments of inertia are given by:

$$I_x^{cs} = I_y^{cs} = \pi\rho kR(R^2 - r^2)\left(\frac{(2k+1)R^2 + r^2}{2}\right) \tag{3}$$

$$I_z^{cs} = \pi\rho kR(R^2 - r^2)(R^2 + r^2) \tag{4}$$

Figure 4 shows the magnitudes of the moments of inertia for a spherical ring and a cylindrical shell ($k = 4$) as a function of the inner radius given by equations 1 and 2. For the spherical ring, I_z is greater than or equal to the transverse moments $I_{x,y}$ for all values of r, while for the cylindrical shell, I_z is less than or equal to the transverse moments $I_{x,y}$ for all values of r. When $r = 0$, the moments of inertia for the spherical ring and cylindrical shell are equivalent to those of a solid sphere and solid cylinder, respectively. Note that while Figure 4B is representative of the high aspect ratio cylindrical rotors commonly used in MAS experiments, when k is low such that the geometry is disk-like, I_z will be greater than $I_{x,y}$ for all values of r.

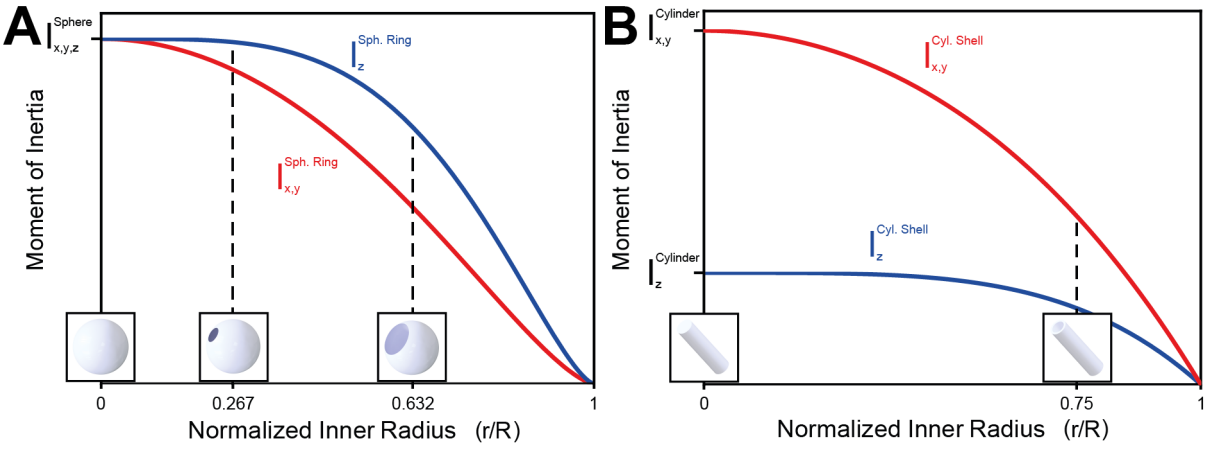

Figure 4. Moments of inertia for spherical and cylindrical rotors as a function of the normalized inner radius r/R. A.) I_z (blue) and $I_{x,y}$ (red) for a spherical rotor as a function of the normalized inner radius. The rotors spun in this study correspond to $r/R = 0.267$. The difference between I_z and $I_{x,y}$ is maximized at $r/R = 0.632$. B.) I_z (blue) and $I_{x,y}$ (red) for a cylindrical rotor with aspect ratio $k = 4$ as a function of the normalized inner radius.

~~An object is capable of spinning stably about any axis without the need for stabilization as long as there are no avenues to dissipate rotational energy. However~~Consider a rigid object with principal moments of inertia I_z, ~~when such dissipative elements~~ I_y, and I_x, rotating about the axis coincident with I_z with a constant angular velocity vector of $(\omega_z, 0, 0)$. If a small

perturbation is applied, the angular velocity vector assumes the form (ω_z, λ, μ). Through substitution of this angular velocity vector into Euler's equations to yield a second order linear differential equation with respect to λ (**??**), we arrive at:

$$\ddot{\lambda} + \frac{(I_z - I_x)(I_z - I_y)}{I_y I_x}\omega_z^2 \lambda = 0 \tag{5}$$

Equation 5 can be used to arrive at the famous result of the intermediate axis theorem, which states that objects with $I_z > I_y > I_x$ will spin stably only about the first and third principal axes (z and x), while a rotation about the second principal axis (y) is unstable. However, for an axially symmetric object, where the axis of symmetry is aligned with the z-axis and $I_y = I_x$ (such as a spherical ring or a cylindrical shell), equation 3 becomes:

$$\ddot{\lambda} + \frac{(I_z - I_x)^2}{I_x^2}\omega_z^2 \lambda = 0 \tag{6}$$

Equation 6 implies that a rotation about the axis of symmetry (z) is always stable, as:

$$\frac{(I_z - I_x)^2}{I_x^2}\omega_z^2 > 0 \tag{7}$$

If, however, the x-axis is instead the axis of symmetry and $I_z = I_y$, equation 5 reduces to $\ddot{\lambda} = 0$, whose solutions grow linearly in time. Thus, rotation about an axis perpendicular to the axis of symmetry is unstable. According to these results, we should expect that a rotation about the axis of symmetry (z) is stable and a rotation perpendicular to the axis of symmetry is unstable, regardless of whether I_z is greater than or equal to I_x.

From this result, we might expect that a spherical shell (axis of symmetry is the highest inertia axis) and a cylindrical shell (axis of symmetry is the lowest inertia axis) to both be continuously stable during a spin about their axis of symmetry. However, it has been observed experimentally that when avenues to dissipate energy are present, ~~the object will~~ an axially-symmetric object can dissipate energy to end up rotating about the axis that minimizes its rotational kinetic energy for a fixed angular momentum, which is the axis with the largest moment of inertia (**???**). This phenomenon has been observed in objects such as comets and asteroids as well as in early spacecraft such as Explorer 1 (**???**). Explorer 1 was a ~~cylindrical~~ cylindrically-symmetric satellite with a high aspect ratio that was meant to spin about its axis of symmetry (the lowest inertia axis) but ended up ~~spinning~~ developing a precession as it transitioned into an end-over-end spin (the highest inertia axis) as a result of energy being dissipated into the structure. ~~Similarly, as a result of this phenomenon, asteroids are more often found tumbling end-over-end rather than spinning about an axis of cylindrical symmetry.~~

~~Like a cylindrical satellite, a high aspect ratio~~ Due to dissipative interactions with the surrounding fluid, a high-aspect-ratio cylindrical MAS rotor ~~requires~~ cannot spin stably and continuously about its axis of symmetry without active stabilization (i.e. ~~, a bearing)in order to spin stably about its axis of symmetry, and any instabilities in the spinning could magnify as the rotor attempts to transition into a spin about its highest inertia axis, potentially leading to a rotor crash~~bearing), as its symmetry axis is also its lowest inertia axis. However, in the case of a spherical MAS rotor, the rotor is placed into the stator without a specific orientation and initially may spin about an arbitrary axis. As the axis of symmetry for a spherical ring is also its greatest inertia

axis, a spherical rotor ultimately ends up stably spinning about its axis of symmetry due to rotational energy being dissipated by interactions with the gas stream and surrounding atmosphere. For this reason, a spherical rotor shows very stable on-axis spinning and resilience to crashing, as ~~any spinning instabilities will be damped by the surrounding fluid and cause the rotor to~~ the rotor will always return to a stable minimum about its axis of symmetry after a perturbation.

~~Equation 1 suggests that spherical rotors~~ Equations 1 and 2 suggest that a spherical rotor should spin most stably about its axis of symmetry, z, when $r/R = 0.632$, where the difference between I_z and $I_{x,y}$ is maximized (Figure 4a). Critically, this means that rotors with a spherical ring geometry can be quite stable even with very large sample volumes. When considering a packed rotor, as long as the density of the caps and sample are lower than the density of the rotor material, I_z will be greater than $I_{x,y}$ for all values of r/R between 0 and 1, and stable on-axis spinning will occur. A detailed investigation of the moments of inertia for a packed spherical rotor taking into consideration the caps, sample and rotor, each with different densities, can be found as an interactive notebook in the supplementary material.

4 Conclusions

While turbine grooves can help to increase MAS rates for spherical rotors, the inertia tensor is responsible for its spinning stability. As MAS rates continue to increase to values in excess of 100 kHz, the possibility of spinning instabilities leading to rotor crashes becomes a significant concern. Spherical rotors spinning at high rates will be able to self-correct to a stable state after a perturbation due to the ~~large~~ highest moment of inertia ~~about their axis~~ axis being aligned with the axis of symmetry. To achieve high MAS rates with spherical rotors, new rotors with smaller outer diameters must be designed and fabricated. These rotors could use shallow, Pelton-style grooves to increase the maximum spinning rate by about 30% compared to a rotor with no machined grooves, as observed here. However, since turbine grooves are not necessary to achieve stable spinning, these rotors could be fabricated without the need for complex micro-machining techniques to produce turbine grooves.

Author contributions. T.O.P. performed the stator, rotor, and probe design, spin test and NMR data collection, the inertia tensor analysis and the writing of the manuscript. A.D. and C.G. fabricated and installed the double-saddle coil and optical tachometer. P.C. assisted with the design process, spin testing, and data collection. L.E.P. assisted with 3D printing of the stators. N.H.A. assisted with the rotor design process. A.B.B. supervised the execution of experiments and guided the writing of the manuscript. All authors contributed to the editing of the manuscript.

Competing interests. A.B.B. is an author on provisional patents related to this work filed by Washington University in Saint Louis (62/703,278 filed on 25 July 2018 and 62/672,840 filed on 17 May 2018). The authors declare no other competing interests.

Code availability. The Mathematica code used to produce the plots seen in Figure 4 as well as an analysis of the inertia tensor as a function of normalized inner radius for a packed spherical rotor with unique densities for the rotor, sample, and caps, may be found in the supplementary information.

Acknowledgements. This research was supported by an NIH Director's New Innovator Award [grant number DP2GM119131] and start-up funding from ETH Zürich. We thank Roland Walker for valuable assistance and advice with 3D printing.